Tetrahedron Letters xxx (2017) xxx–xxx

Contents lists available at ScienceDirect

Tetrahedron Letters

journal homepage: www.elsevier.com/locate/tetlet

Novel fluorescent probe bearing triarylimidazole and pyridine moieties for the rapid and naked-eye recognition of Cu^{2+}

Shuzhi Liu, Yijiang Liu *, Hua Pan, Hongbiao Chen, Huaming Li *

College of Chemistry, Xiangtan University, Xiangtan 411105, Hunan Province, China

ARTICLE INFO

Article history:
Received 28 September 2017
Revised 28 November 2017
Accepted 30 November 2017
Available online xxxx

Keywords:
Fluorescent probe
Triarylimidazole
Cu^{2+}detection
High sensitivity
Reversibility

ABSTRACT

A new fluorescent probe (TPIP) bearing triarylimidazole and pyridine moieties was synthesized and applied to the detection of Cu^{2+} with high sensitivity and selectivity. Upon the addition of Cu^{2+}, the probe displayed an apparent dual-channel signal change of the UV–Vis absorption and fluorescence spectra, and the obvious color change from bright blue to colorless under a UV lamp was discernable to the naked eye. The sensing mechanism of the probe towards Cu^{2+} was verified to be *via* complexation, and the binding reaction was rapidly complete within 30 s. Good linearity was observed between the probe and Cu^{2+}, and the detection limit was calculated to be 1.96×10^{-8} M. The reversibility of the probe was easily achieved by adding EDTA, which released the free probe with over 95% fluorescence recovery. Furthermore, the recognition of Cu^{2+} on TLC plates was realized, indicating the potential utility of the probe.

Introduction

The design and synthesis of small molecule fluorescent probes for the detection of various metal ions has attracted considerable attention in the fields of chemical, biological and environmental analysis.[1–3] Among metal ions, the recognition of Cu^{2+} has received considerable interest in the past decades due to its crucial psychological function in the human body.[4–6] As the third most important trace element (besides Fe^{2+} and Zn^{2+}), Cu^{2+} participates in the catalytic reactions of a variety of metalloenzymes, which are involved in the processes of cell respiration, electron transfer and oxidation, neurotransmitter biosynthesis and degradation, and signal transduction.[7,8] Consequently, the disturbance of cellular homeostasis of Cu^{2+} may result in serious diseases. For example, deficient Cu^{2+} intake increases the risk of leucoderma, arthritis and anemia, while excessive Cu^{2+} levels can cause neurodegenerative diseases such as Alzheimer's and Parkinson's, genetic disorders including Menkes and Wilson's diseases, and even influence tumour growth.[9–12] The extensive use and the easy diffusion of Cu^{2+} increase the likelihood of Cu^{2+}-related contamination. Therefore, the recognition of trace amounts of Cu^{2+} has attracted tremendous attention in recent years.

The use of fluorescent probes has stood out from the traditional methods of atomic absorption spectrometry (AAS), inductively coupled plasma-atomic emission spectroscopy (ICP-AES) and electrochemical methods due to the merits of simple operation, low cost, high sensitivity and real-time analysis.[13–16] The two main strategies for fluorescent Cu^{2+} probes are Cu^{2+}-promoted "reactive" probes and "complexation" probes. The "reactive" probes are noted for their high selectivity, but the reaction processes are time-consuming and usually suffer from strict reaction conditions.[17–20] The "complexation" probes containing N, O, and S atoms in their molecular structures usually display fluorescent quenching behavior, and are reversible with the addition of Cu^{2+} complexing ligands, such as EDTA and S^{2-}.[21,22] For example, Gupta and co-workers reported an imidazoazine-based fluorescent probe, which could be regenerated with 90% fluorescence recovery upon the addition of EDTA, and retaining the same level of efficiency in the reused probe.[23] Additionally, Meng and co-workers developed an "off-on" fluorescent probe based on a rhodamine B derivative, where the addition of EDTA could interact with Cu^{2+} thus releasing the probe with an obvious color change in sunlight.[24] Furthermore, fluorescein-, benzoyl hydrazone-, and benzimidazole-based fluorescent probes have also been applied for the reversible detection of Cu^{2+}.[25–27] Therefore, the development of novel fluorescent Cu^{2+} probes with high sensitivity and reversibility is still highly desirable.

Triarylimidazole derivatives are well-known fluorophores owing to their extended conjugated-system structure, high molar absorption coefficient and good photochemical properties, and have been applied as fluorescent probes.[28,29] Recently, we reported a novel compound containing the triarylimidazole chromophore (TPI-H) to sequentially detect Cu^{2+} and S^{2-} with a detection limit

* Corresponding authors.
E-mail addresses: liuyijiang84@163.com (Y. Liu), lihuaming@xtu.edu.cn (H. Li).

https://doi.org/10.1016/j.tetlet.2017.11.059
0040-4039/

at the nanomole level.[30] Meanwhile, an azoaniline-arylimidazole dyad was synthesized to detect Cu^{2+} with high sensitivity based on the Cu^{2+}-catalyzed oxidative cyclization.[31] Given the good performance of triarylimidazole-based fluorescent probes, herein, we report the synthesis of a new triarylimidazole-pyridine based fluorescent probe (TPIP), which can be applied to detect Cu^{2+} with high sensitivity and selectivity, rapid response and a visible color change based on the complexation mechanism. The probe could also be easily regenerated by adding EDTA with excellent fluorescence recovery.

Results and discussion

Synthesis and characterization of TPIP

The probe (TPIP) was synthesized *via* a two-step route as shown in Scheme 1. First, 4-(4,5-diphenyl-1*H*-imidazole-2-yl)benzaldehyde (**1**) was synthesized according to a reported literature procedure.[32] Next, an efficient one-pot dehydrogenative cross-coupling between compound **1** and 2-aminopyridine proceeded under CuI catalysis in DMF, affording the target molecule TPIP in 70% yield as a pale-yellow solid. The molecular structure of TPIP was characterized by ^{1}H NMR (ESI, Fig. S1), ^{13}C NMR (ESI, Fig. S2) and MALDI-TOF mass spectrum (ESI, Fig. S3). The probe was soluble in common organic solvents, and the solvent mixture $CHCl_3/CH_3OH$ (8/2, v/v) was selected for further experiments.

Absorption and fluorescence response of TPIP towards Cu^{2+}

The UV–Vis absorption titration of the probe with various amounts of Cu^{2+} was initially investigated. As shown in Fig. 1a, the probe in $CHCl_3/CH_3OH$ (20 μM, 8/2, v/v) showed two absorption bands centered at 290 nm and 345 nm, which might be attributed to the corresponding pyridine moiety and triarylimidazole moiety. The absorbance of both peaks gradually decreased upon the addition of Cu^{2+}, indicating that the energy levels of the molecule were changed due to coordination between TPIP and Cu^{2+}. The absorption profile remained unchanged when 0.5 equivalents of Cu^{2+} was introduced, suggesting a 2:1 complex between TPIP and Cu^{2+} was achieved. The linear response of TPIP as a function of Cu^{2+} concentration was observed in the range of 0–10 μM (inset Fig. 1a). The association constant (K_a) determined from the UV–Vis titration was calculated to be 8.5×10^{-4}. Upon excitation at 280 nm, the free TPIP displayed a distinct emission peak centered at 436 nm. The fluorescent intensity at 436 nm gradually decreased with increasing amounts of Cu^{2+}, which quenched 98.2% of the fluorescence and stabilized upon the addition of 0.5 equivalents of Cu^{2+} (Fig. 1b). The continuous color change of the TPIP solution from bright blue to colorless under a UV lamp was observable to the naked eye (inset Fig. 1c). It is clearly indicated that the fluorescent intensity is linear to the Cu^{2+} amount in the range of 0–10 μM with a correlated coefficient of 0.995, which facilitated the quantitative detection of Cu^{2+} (Fig. 1c). The detection limit was calculated to be 1.96×10^{-8} M based on the equation DL = 3σ/S, which was far lower than the permissive level of Cu^{2+} (20 μM) assigned by the U.S. Environmental Protection Agency (EPA).

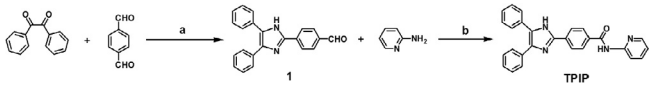

Scheme 1. Synthetic route towards TPIP: (a) CH_3COONH_4, CH_3COOH, reflux, 4 h, 81%; (b) CuI (10 mol%), DMF, 80 °C, 24 h, 70%.

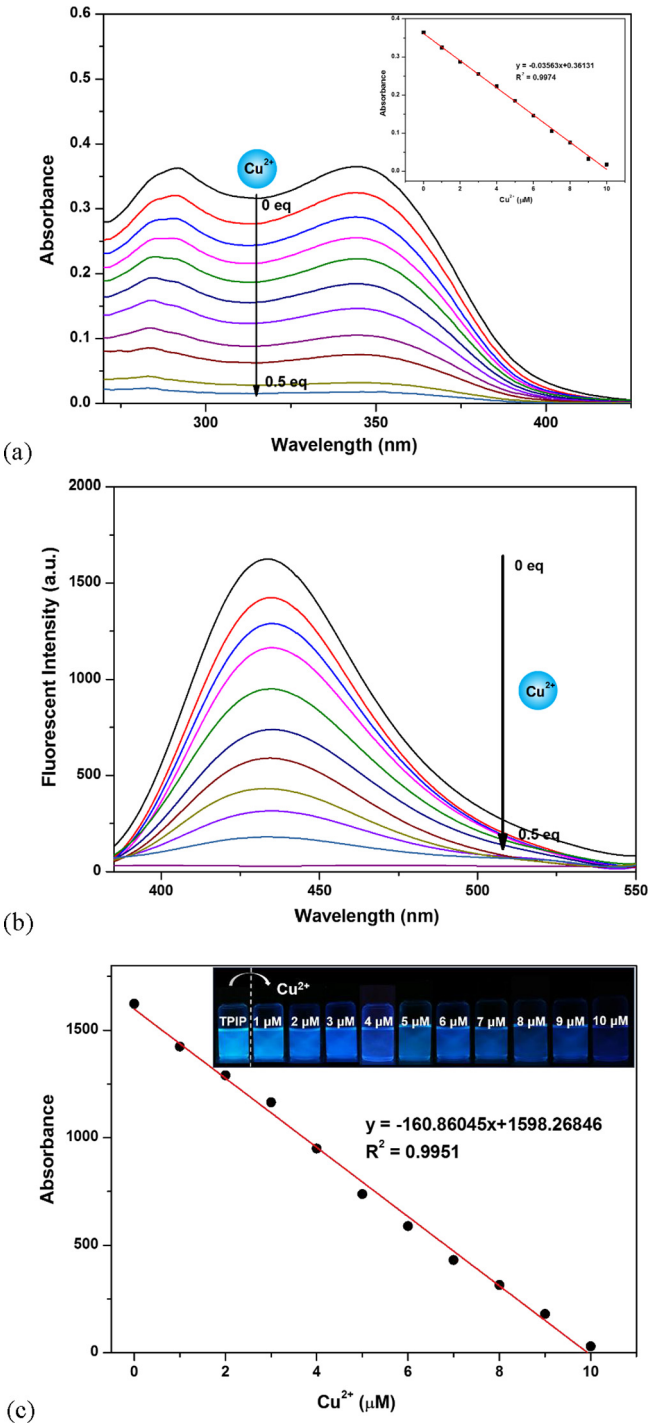

Fig. 1. (a) Absorption spectra and (b) fluorescence spectra (λ_{ex}, 280 nm) of a TPIP solution (20 μM, $CHCl_3$/MeOH, 8/2, v/v) responding to various concentrations of Cu^{2+} (0, 0.05, 0.10, 0.15, 0.20, 0. 25, 0.30, 0.35, 0.40, 0.45 and 0.50 eq.), inset (a) Plot of TPIP absorbance at A_{345} as a function of Cu^{2+} concentration; (c) Plot of TPIP fluorescent intensity at F_{436} as a function of Cu^{2+} concentration, inset photographs of the TPIP solutions with various amount of Cu^{2+} under a UV lamp.

Selectivity and competitiveness of TPIP towards Cu^{2+}

The selectivity of a fluorescent probe is an important property. Thus, the selective coordination between TPIP and Cu^{2+} was studied by fluorescence spectroscopy with various metal ions, including Zn^{2+}, Na^+, K^+, Ni^{2+}, Mn^{2+}, Ca^{2+}, Co^{2+}, Pb^{2+}, Ba^{2+}, Hg^{2+}, Mg^{2+}, Fe^{3+}, Fe^{2+} and Cu^{2+}. As shown in Fig. 2a, no obvious fluorescence quenching effect was observed when 50 μM of Zn^{2+}, Na^+, K^+, Ni^{2+}, Mn^{2+}, Ca^{2+},

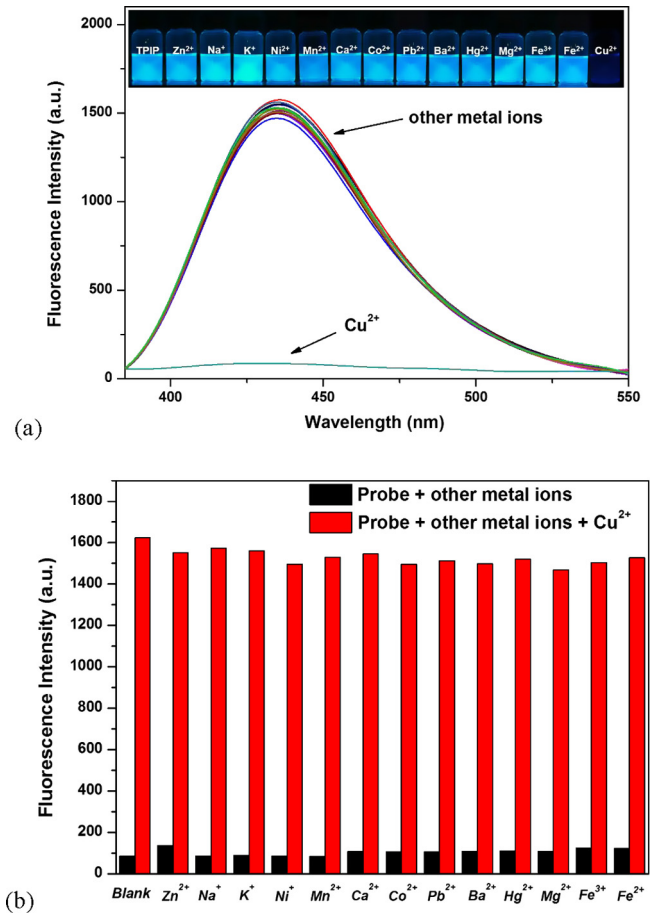

Fig. 2. (a) Fluorescence spectra (λ_{ex}, 280 nm) of a TPIP solution (20 μM, $CHCl_3$/MeOH, 8/2, v/v) upon the addition of other metal ions (each 50 μM) and Cu^{2+} (10 μM), inset photographs of the mixtures under a UV lamp; (b) Fluorescence response of a TPIP solution (20 μM, $CHCl_3$/MeOH, 8/2, v/v) with other metal ions (red bar, each 50 μM) and in the presence of other metal ions (50 μM) together with Cu^{2+} (10 μM) (black bar).

Co^{2+}, Pb^{2+}, Ba^{2+}, Hg^{2+}, Mg^{2+}, Fe^{3+} and Fe^{2+} were introduced to the TPIP solution, and the solution color remained bright blue under a UV lamp (inset Fig. 2a). In contrast, the addition of 10 μM of Cu^{2+} induced almost complete fluorescence quenching, and the bright blue solution changed to almost colorless. Furthermore, the competitiveness of TPIP binding with Cu^{2+} was investigated in the presence of various other metal ions. The fluorescent intensity was recorded when Cu^{2+} was sequentially added to various solutions of TPIP and a metal ion. The results showed that the manner of the fluorescence quenching of the mixture was the same as Cu^{2+}, demonstrating that the quenching effect of Cu^{2+} to TPIP was not affected by competitive metal ions (Fig. 2b). These results clearly demonstrated the high selectivity and competitiveness of TPIP towards Cu^{2+}. Furthermore, the influence of anionic counterions on the fluorescence response of TPIP towards Cu^{2+} was measured. The variation of fluorescent intensity (F-F_0) of TPIP upon the addition of different copper salts, such as $Cu(CH_3COO)_2$, $CuSO_4$, $Cu(NO_3)_2$ and $CuCl_2$, is shown in Fig. S4. Similar fluorescence quenching behavior was observed using different copper salts, suggesting a negligible effect of the counter anion on the detection of Cu^{2+} using the probe.

Response time of TPIP towards Cu^{2+}

The rapid response of a probe to an analyte is a crucial factor to evaluate the performance. In this study, the binding kinetics of TPIP towards Cu^{2+} was investigated using time-dependent fluorescence spectra. As shown in Fig. 3, the fluorescent intensity of TPIP at 436 nm was quickly quenched (within 30 s) upon the addition of Cu^{2+}, reaching a minimum intensity that remained unchanged even though the reaction time was extended to 300 s. This phenomenon indicated that the binding reaction between TPIP and Cu^{2+} was extremely rapid and complete within 30 s under the experimental conditions. Therefore, the probe could potentially be used as an effective method for real-time analysis.

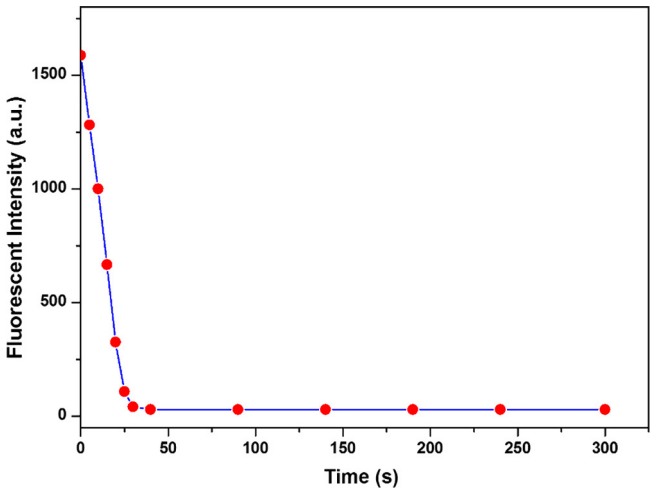

Fig. 3. Reaction-time profile of TPIP (20 μM, $CHCl_3$/MeOH, 8/2, v/v) in the presence of Cu^{2+} (10 μM).

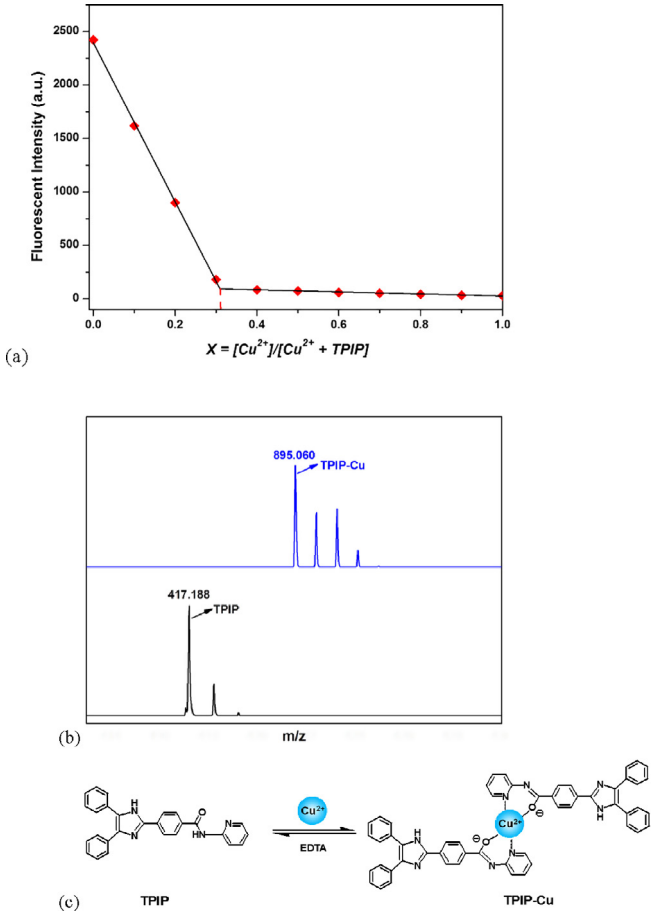

Fig. 4. (a) Job's fluorescence titration plot of a TPIP solution with Cu^{2+} in $CHCl_3$/MeOH (8/2, v/v); (b) MALDI-TOF mass spectrum of TPIP (black line) and TPIP-Cu (blue line); (c) Proposed binding mode between TPIP and Cu^{2+}.

Proposed mechanism of TPIP binding towards Cu^{2+}

To further clarify the binding mechanism, Job's titration, mass spectrometry and FT-IR spectroscopy were performed, while the NMR for the complexation was not available due to the paramagnetic property of Cu^{2+}.[33] Firstly, the Job's titration was carried out by maintaining the total concentration of TPIP and Cu^{2+} at 40 μM and changing the molar ratio of $[Cu^{2+}]/[TPIP]$ in $CHCl_3$/MeOH (8/2, v/v) through fluorescence spectroscopy. The fluorescent intensity of TPIP showed the minimum intensity at 436 nm when the molar fraction of Cu^{2+} was close to 33%, which indicated that a 2:1 stoichiometry was possible for the binding mode of TPIP and Cu^{2+} (Fig. 4a). The MALDI-TOF mass spectrum of the isolated complex also supported the 2:1 stoichiometry with an *m*/*z* peak at 859.060 equal to $[2TPIP + Cu^{2+} - 2H]$ (Fig. 4b). Furthermore, the FT-IR spectra of TPIP and TPIP-Cu were measured in KBr disks and the corresponding curves are shown in Fig. S5. The distinct characteristic peak of an amide carbonyl located at 1651 cm^{-1} in TPIP disappeared, and a new peak appeared at 1617 cm^{-1}. This suggested that the amide carbonyl was involved in the coordination with Cu^{2+}. Therefore, the plausible binding mode between TPIP and Cu^{2+} was proposed as shown in Fig. 4c.

Reversibility of TPIP

For practical applications, the reversibility of the probe is a significant factor. To examine whether the probe is recyclable and reusable, the sodium salt of ethylendiaminetetraacetic acid (EDTA) was added to the TPIP-Cu complex solution as a sequestering agent. As shown in Fig. 5, upon the addition of EDTA (0.5 eq.), over 95% fluorescence was recovered. Meanwhile, the fluorescence color of the solution underwent a distinct change from colorless to bright blue (inset Fig. 5). Additionally, the isolated product from the reaction of TPIP-Cu and EDTA was collected and purified by column chromatography, which was confirmed to be free TPIP by ^1H NMR spectroscopy (ESI, Fig. S6). These results clearly suggested that the probe was released from the complex, indicating that it is recyclable and reusable.

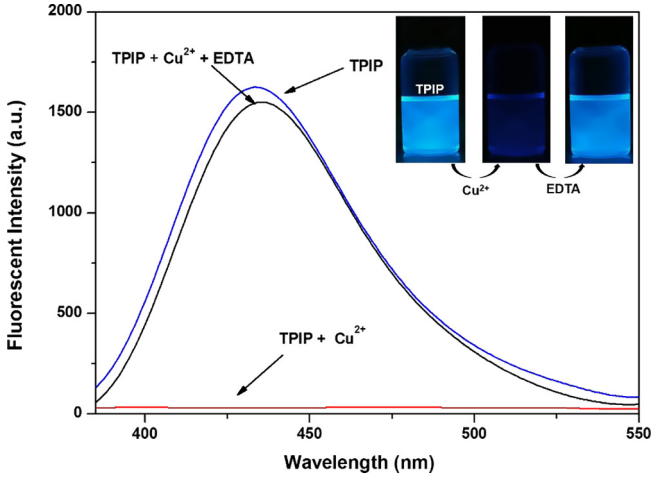

Fig. 5. Fluorescence spectra of the probe, TPIP + Cu^{2+} and TPIP + Cu^{2+} + EDTA in $CHCl_3$/MeOH (8/2, v/v), inset corresponding photographs of the solutions under a UV lamp.

Practical application of TPIP

Based on the distinct fluorescence color change of the probe solution upon the addition of Cu^{2+}, TLC plates coated with TPIP was proposed to detect Cu^{2+}. As shown in Fig. 6, TPIP coated TLC plates displayed blue fluorescence. When the TPIP coated TLC plates were further immersed into different concentrations of Cu^{2+} solution, gradual fluorescence color changes were observed under a UV lamp. However, no color changes were observed when TPIP coated TLC plates were further immersed in other common metal ions solutions, such as Pb^{2+}, Hg^{2+}, Ca^{2+}, K^+ and Na^+, and still exhibited blue fluorescence. Additionally, when different concentrations of Cu^{2+} aqueous media and other common metal ions aqueous media were used, the TPIP coated TLC plates exhibited similar color changes as mentioned above (ESI, Fig. S7). This phenomenon indicates that the probe has potential utility in the detection of Cu^{2+} in the solid state, which represents more portable and convenient detection conditions.

Conclusion

In summary, a fluorescent probe bearing a triarylimidazole moiety and a pyridine moiety was synthesized and characterized by ^1H NMR and ^{13}C NMR spectroscopy as well as MALDI-TOF mass spectrometry. The probe was applied to monitor Cu^{2+} in $CHCl_3$/MeOH (8/2, v/v), which displayed rapid response and remarkable fluorescent quenching upon binding with Cu^{2+}, with a distinct color change from bright blue to colorless which was discernable to the naked eye. The variation of fluorescent intensity was linear with Cu^{2+}, and the detection limit was 1.96×10^{-8} M. The 2:1 binding mode between TPIP and Cu^{2+} was verified by Job's fluorescence titration, MALDI-TOF mass spectroscopy and FT-IR spectroscopy. The binding reaction between TPIP and Cu^{2+} was extremely rapid and complete within 30 s, indicating significant potential for real-time analysis. The investigation on the reversibility of the probe demonstrated that it was simple to regenerate the probe by the addition of EDTA, which recovered 95% fluorescence. Furthermore, the recognition of Cu^{2+} on TLC plates was also successfully realized, suggesting the practical application of the TPIP probe.

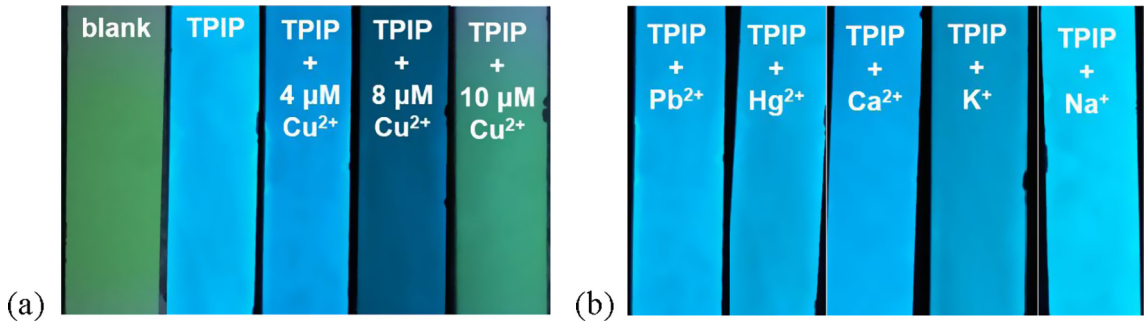

Fig. 6. (a) Photographs of TPIP coated TLC plates immersed in different concentrations of Cu^{2+}; (b) Photographs of the TLC plates immersed in TPIP solution in the presence of other metal ions (Pb^{2+}, Hg^{2+}, Ca^{2+}, K^{2+} and Na^{2+}).

Please cite this article in press as: Liu S., et al. Tetrahedron Lett. (2017), https://doi.org/10.1016/j.tetlet.2017.11.059

Acknowledgements

This study was financially supported by National Natural Science Foundation of China (NSFC 51603177), China Postdoctoral Science Foundation (2017M612571) and the Opening Foundation of the Key Laboratory of Creative Platform of the Education Department of Hunan Province, China.

A. Supplementary data

Supplementary data associated with this article can be found, in the online version, at https://doi.org/10.1016/j.tetlet.2017.11.059.

References

1. Lee MH, Kim JS, Sessler JL. *Chem Soc Rev*. 2015;44:4185–4191.
2. Vendrell M, Zhai DT, Er JC, Chang YT. *Chem Rev*. 2012;112:4391–4420.
3. Su W, Gu B, Hu XJ, et al. *Dyes Pigments*. 2017;137:293–298.
4. Cotruvo Jr JA, Aron AT, Ramos-Torres KM, Chang CJ. *Chem Soc Rev*. 2015;44:4400–4414.
5. Liu S, Wang YM, Han J. *J Photochem Photobiol C*. 2017;32:78–103.
6. Niu CX, Song QW, He G, Na N, Ouyang J. *Anal Chem*. 2016;88:11062–11069.
7. Culotta VC, Yang M, O'Halloran TV. *BBA*. 2006;1763:747–758.
8. Uauy R, Olivares M, Gonzalez M. *Am J Clin Nutr*. 1998;67:952S–959S.
9. Tiffany-Castiglioni E, Hong S, Qian YC. *Int J Dev Neurosci*. 2011;29:811–818.
10. Rossi L, Lombardo MF, Ciriolo MR, Rotilio G. *Neurochem Res*. 2004;29:493–504.
11. Muthaup G, Schlicksupp A, Hess L, et al. *Science*. 1996;271:1406–1409.
12. Barnham KJ, Masters CL, Bush AI. *Nat Rev Drug Discovery*. 2004;3:205–214.
13. Yin BC, Zuo P, Huo H, Zhong XH, Ye BC. *Anal Biochem*. 2010;401:47–52.
14. Gonzales APS, Firmino MA, Nomura CS, Rocha FRP, Oliveira PV, Gaubeur I. *Anal Chim Acta*. 2009;636:198–204.
15. Becker JS, Matusch A, Depboylu C, Dobrowolska J, Zoriy MV. *Anal Chem*. 2007;79:6074–6080.
16. Li DX, Sun X, Huang JM, et al. *Dyes Pigments*. 2016;125:18–191.
17. Li D, Sun X, Wang M, et al. *Sensors Actuators B*. 2015;220:1006–1016.
18. Long LL, Wu YJ, Wang L, Gong AH, Hu RF, Zhang C. *Anal Chim Acta*. 2016;908:1–7.
19. Wang Y, Mao PD, Wu WN, et al. *Sensors Actuators B*. 2017;251:813–820.
20. Huo FJ, Yin CX, Yang YT, Su J, Chao JB, Liu DS. *Anal Chem*. 2012;84:2219–2223.
21. Li G, Tao FR, Wang H, Li YC, Wang LP. *Sensors Actuators B*. 2015;211:325–331.
22. Hu Y, Zhang J, Lv YZ, Huang XH, Hu SL. *Spectrochim Acta A*. 2016;157:164–169.
23. Kumawat LK, Kumar M, Bhatt P, Sharma A, Asif M, Gupta VK. *Sensors Actuators B*. 2017;240:365–375.
24. Meng XF, Xu YX, Liu JL, Sun LN, Shi LY. *Anal Methods*. 2016;8:1044–1051.
25. Wu X, Gong XJ, Dong WJ, et al. *RSC Adv*. 2016;6:59677–59683.
26. Anbu S, Ravishankaran R, Silva MFCG, Karande AA, Pombeiro AJL. *Inorg Chem*. 2014;53:6655–6664.
27. Tang LJ, Cai MJ, Huang ZL, et al. *Sensors Actuators B*. 2013;185:188–194.
28. Yagi K, Soong CF, Irie M. *J Org Chem*. 2001;66:5419–5423.
29. Zhao B, Xu Y, Ma MJ, Kan W, Deng QG. *Res Chem Intermed*. 2015;41:8031–8040.
30. Wang YP, Qiu DL, Li MN, Liu YJ, Chen HB, Li HM. *Spectrochim Acta A*. 2017;185:256–262.
31. Wang YP, Liu SZ, Chen HB, Liu YJ, Li HM. *Dyes Pigments*.. 2017;142:293–299.
32. Zheng W, He XZ, Chen HB, Gao Y, Li HM. *Spectrochim Acta A*. 2014;124:97–101.
33. Helal A, Rashid MHO, Choi CH, Kim HS. *Tetrahedron*. 2011;67:2794–2802.